

# Lawrence Berkeley National Laboratory

## Recent Work

### Title

Cage-Walking: Vertex Differentiation by Palladium-Catalyzed Isomerization of B(9)-Bromo-meta-Carborane.

### Permalink

<https://escholarship.org/uc/item/0x57v855>

### Journal

Journal of the American Chemical Society, 139(23)

### ISSN

0002-7863

### Authors

Dziedzic, Rafal M  
Martin, Joshua L  
Axtell, Jonathan C  
[et al.](#)

### Publication Date

2017-06-01

### DOI

10.1021/jacs.7b04080

Peer reviewed

# Cage-Walking: Vertex Differentiation by Palladium-Catalyzed Isomerization of B(9)-Bromo-*meta*-Carborane

Rafal M. Dziejdzic,<sup>†</sup> Joshua L. Martin,<sup>†</sup> Jonathan C. Axtell,<sup>†</sup> Liban M. A. Saleh,<sup>†</sup> Ta-Chung Ong,<sup>†</sup> Yun-Fang Yang,<sup>†</sup> Marco S. Messina,<sup>†</sup> Arnold L. Rheingold,<sup>‡</sup> K. N. Houk,<sup>†</sup> and Alexander M. Spokoyny<sup>\*,†,§</sup>

<sup>†</sup>Department of Chemistry and Biochemistry, University of California, Los Angeles, 607 Charles E. Young Drive East, Los Angeles, California 90095, United States

<sup>‡</sup>Department of Chemistry and Biochemistry, University of California, San Diego, 9500 Gilman Drive, La Jolla, California 92093, United States

<sup>§</sup>California NanoSystems Institute (CNSI), University of California, Los Angeles, 570 Westwood Plaza, Los Angeles, California 90095, United States

## Supporting Information

**ABSTRACT:** We report the first observed Pd-catalyzed isomerization (“cage-walking”) of B(9)-bromo-*meta*-carborane during Pd-catalyzed cross-coupling, which enables the formation of B–O and B–N bonds at all boron vertices (B(2), B(4), B(5), and B(9)) of *meta*-carborane. Experimental and theoretical studies suggest this isomerization mechanism is strongly influenced by the steric crowding at the Pd catalyst by either a biaryl phosphine ligand and/or substrate. Ultimately, this “cage-walking” process provides a unique pathway to preferentially introduce functional groups at the B(2) vertex using B(9)-bromo-*meta*-carborane as the sole starting material through substrate control.

Isomerization mechanisms such as chain-walking via  $\beta$ -hydride elimination/reinsertion and aryne-based rearrangements (Figure 1A) are ubiquitous in metal-catalyzed transformations of organic molecules.<sup>1,2</sup> Through judicious choice of catalyst design, these mechanistic pathways can be biased to form specific regioisomers. Thus, metal-catalyzed isomerization

control can provide a means of incorporating functional groups in molecules at positions remote from where initial bond activation occurs.<sup>1–3</sup>

Boron clusters are unique molecular scaffolds that feature three-dimensional (3D) electronic delocalization.<sup>4</sup> Specifically, in the case of icosahedral carboranes (C<sub>2</sub>B<sub>10</sub>H<sub>12</sub>) this delocalization is nonuniform.<sup>5</sup> This charge distribution makes carboranes an interesting alternative to classical carbon-based structural building blocks such as aryl and alkyl groups.<sup>6</sup> Because of their inherent robustness, carboranes can be promising molecular building blocks for applications ranging from pharmacophores to photoactive materials.<sup>7</sup> Ultimately, vertex-specific functionalization routes (vertex differentiation) are critical for constructing carborane-containing molecules and materials.<sup>7,8</sup>

Recent developments in carborane functionalization have relied on several metal-catalyzed routes, including B–H activation (either directed or undirected) and cross-coupling of halogenated carborane electrophiles at both C and B vertices.<sup>8,9</sup> Even so, these approaches provide limited access to rational, vertex-specific B–H functionalization. Surprisingly, metal-catalyzed isomerization reactivity commonly observed with classical organic substrates (*vide supra*) has never been reported for any boron cluster systems, including carboranes. Herein we disclose our discovery of a Pd-catalyzed activation of B(9)-bromo-*meta*-carborane (Br–B(9)), which can undergo subsequent “cage-walking”, leading to the formation of B(2)-, B(4)-, B(5)-, and B(9)-functionalized clusters in the presence of a suitable nucleophile (Figure 1B).

Recently we reported the Pd-catalyzed cross-coupling of Br–B(9) to generate B(9)–O and B(9)–N bonds with a wide range of substrates.<sup>9</sup> This cross-coupling relied on biaryl phosphine ligands to generate monoligated palladium(0) species ([LPd]) capable of undergoing oxidative addition into the B–Br bond of Br–B(9). To our surprise, during the course of subsequent investigations, when the DavePhos (L1) or SPhos (L2) ligand was replaced with the bulkier XPhos

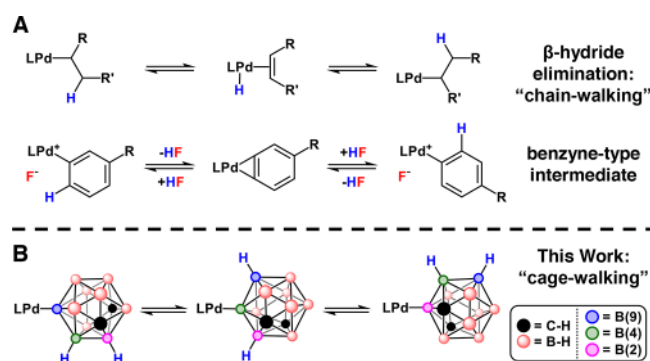


**Figure 1.** (A) Pd-catalyzed olefin isomerization through  $\beta$ -hydride elimination and arene regioisomer formation through a proposed benzyne intermediate. (B) Pd-catalyzed isomerization of *meta*-carboranyl through “cage-walking”.

Received: April 25, 2017

Published: May 25, 2017

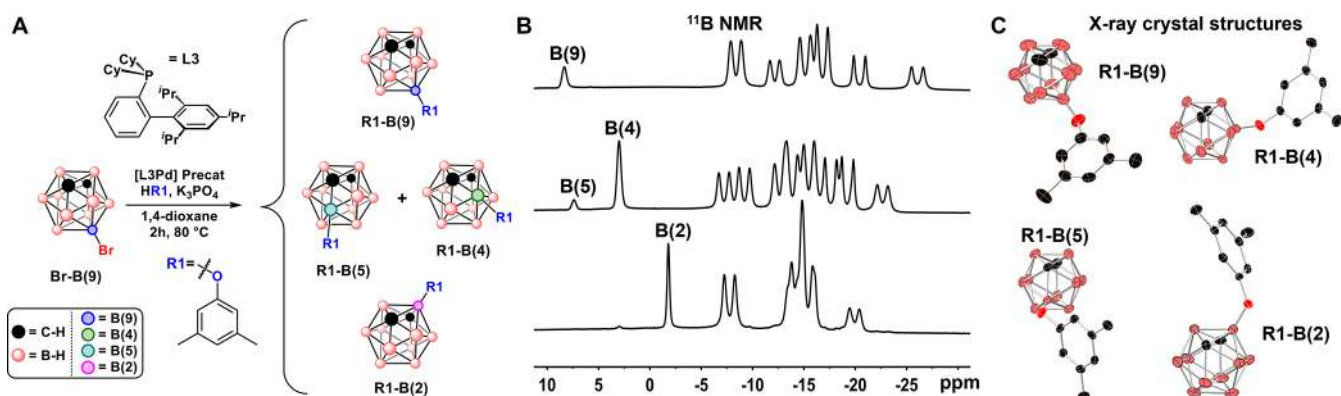


**Figure 2.** (A) Reaction conditions that result in the formation of **R1-*meta*-carborane** regioisomers. (B)  $^{11}\text{B}$  NMR spectra of the isolated regioisomers. Singlet resonances (no  $^{11}\text{B}$ – $^1\text{H}$  coupling) corresponding to the B–O-bonded vertex are labeled; all other resonances correspond to doublet resonances arising from  $^{11}\text{B}$ – $^1\text{H}$  couplings. (C) Single-crystal X-ray structures of **R1-B(*n*)**, *n* = 2, 4, 5, 9 (ellipsoids drawn at 50% probability and H atoms omitted for clarity).

congener (**L3**) in the presence of alcohol or amine substrates, we consistently observed not one but rather three distinct peaks with identical *m/z* by gas chromatography–mass spectrometry (GC–MS). For example, using 3,5-dimethylphenol (**R1**) as a cross-coupling partner with **Br-B(9)**, we observed several products with identical *m/z* (see the [Supporting Information](#) (SI)). Upon chromatographic separation of the reaction mixture on silica gel, we identified four distinct **R1-carborane** compounds by  $^{11}\text{B}$ ,  $^1\text{H}$ , and  $^{13}\text{C}$  NMR spectroscopy ([Figure 2](#)).

The isolated carborane-containing molecules show a distinct downfield singlet in the  $^{11}\text{B}$  NMR spectrum corresponding to **R1** bound at a B(2), B(4), B(5), or B(9) vertex of *meta*-carborane (**R1-B(2)**, **R1-B(4)**, **R1-B(5)**, and **R1-B(9)**, respectively). Although we were unable to chromatographically separate **R1-B(5)** and **R1-B(4)**, we identified the isomer ratio as 15:85 by  $^{11}\text{B}$  and  $^1\text{H}$  NMR spectroscopy: **R1-B(4)** is  $C_1$ -symmetric, resulting in 10  $^{11}\text{B}$  NMR resonances (one singlet and nine doublets), whereas **R1-B(5)** contains a mirror plane, resulting in six  $^{11}\text{B}$  NMR resonances (one singlet and five doublets). Thus, the more intense singlet at  $\sim 3$  ppm ([Figure 2B](#)) is assigned to the dominant pattern of **R1-B(4)**. Similarly, two sets of  $^1\text{H}$  and  $^{13}\text{C}$  NMR resonances corresponding to **R1-B(5)** and **R1-B(4)** were observed in a 15:85 signal ratio for the CH aromatic and aliphatic regions, respectively (see the [SI](#)). These structural assignments are further supported by single-crystal X-ray diffraction studies of the four regioisomers ([Figure 2C](#)). Interestingly, **R1-B(4)** is the only monofunctionalized *meta*-carborane regioisomer that exhibits chirality. **R1-B(4)** crystallized as two distinct polymorphs, with both polymorphs containing equal amounts of the two enantiomers in the unit cell. Chiral HPLC analysis further supports the presence of two **R1-B(4)** enantiomers in the isolated mixture ([Figure S12](#)).

To further assess the generality of this isomerization process, we examined three biaryl phosphine ligands and several substrates to generate B–O- and B–N-bound carborane regioisomers ([Figure 3](#)). Consistent with our previous report, [**L1Pd**] and [**L2Pd**] generate B(9) isomers almost exclusively with O- and N-based nucleophiles.<sup>9</sup> However, [**L3Pd**] generates appreciable amounts of regioisomers under the same conditions. Noteworthy was the presence of bromo-*meta*-carborane regioisomers when the cross-coupling reactions were stopped early, indicating that isomerization of **Br-B(9)** occurs in addition to the cross-coupling reaction. Furthermore, **Br-B(9)** forms bromo-*meta*-carborane isomers in the presence

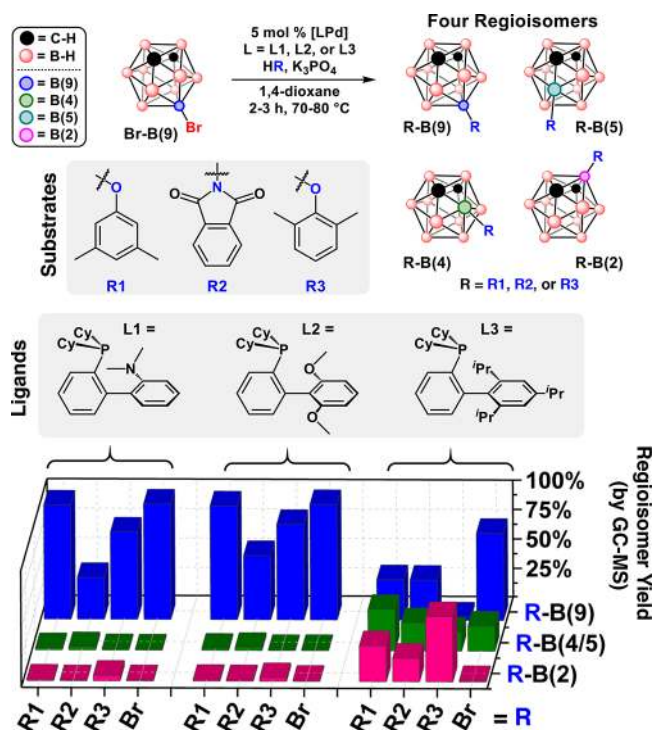


**Figure 3.** Reaction conditions for forming B-functionalized *meta*-carborane isomers using different substrates (**R1**–**R3**) and biaryl phosphine ligands (**L1**–**L3**). Yields were obtained by GC–MS. See the [SI](#) for full experimental conditions.

of [**L3Pd**] precatalyst and triethylamine, implying that isomerization can occur prior to transmetalation of a cross-coupling partner and subsequent reductive elimination of the B-functionalized *meta*-carborane. Hence, this metal-catalyzed isomerization may provide a convenient pathway to B(2)-, B(4)-, and B(5)-functionalized *meta*-carborane species that circumvents laborious and often low-yielding protocols such as deboronation/capitulation or thermal isomerization strategies.<sup>10,11</sup>

Since bromo-*meta*-carboranyl isomerization can occur before all of the carborane regioisomers are depleted by cross-coupling (*vide supra*), we hypothesized that the isomerization process might operate separately from the main cross-coupling cycle. To further explore the isomerization mechanics, we attempted

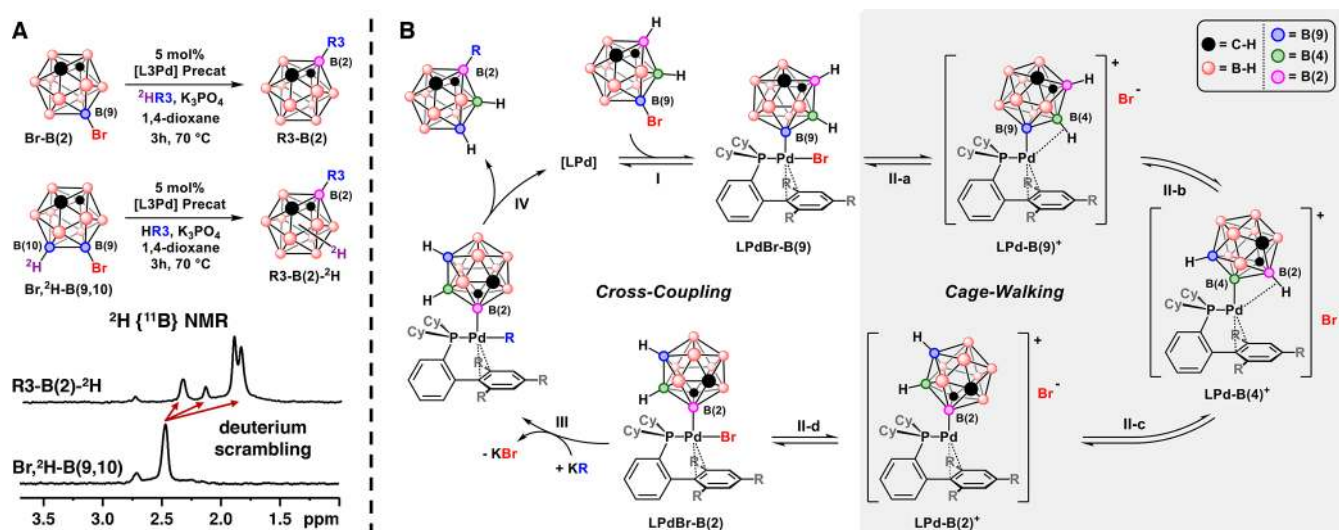


**Figure 4.** (A) Deuterium labeling experiments. The resonance at 2.7 ppm is present from polydeuterated  $\text{Br-B}(9)$ . See the SI for full experimental details. (B) Proposed metal-catalyzed isomerization of bromo-*meta*-carborane through a “cage-walking” mechanism: (I) oxidative addition; (II-a) bromide dissociation; (II-b, II-c) “cage-walking”; (II-d) bromide association; (III) transmetalation; (IV) reductive elimination.

to inhibit transmetalation by increasing the steric bulk of the cross-coupling partner, thereby allowing the active catalyst species to operate in the isomerization pathway for a longer time (Figure 4, step II). Indeed, cross-coupling reactions using bulky L3 and sterically congested 2,6-dimethylphenol (R3) yielded R3-B(2) as the major product (Figure 3). As a control experiment, equimolar amounts of 3,5-dimethylphenol (R1) and 2,4,6-trimethylphenol (R3', a variant of R3 to permit separation of the products by GC-MS) were reacted with Br-B(9) in the presence of [L3Pd] and  $\text{K}_3\text{PO}_4$  in 1,4-dioxane at 80 °C (Figures S5 and S6). GC-MS analysis of the reaction mixture showed complete consumption of Br-B(9) with R1-*meta*-carborane isomers as the major products, suggesting that the size of the nucleophile is linked to the rate of product formation. Since oxidative addition is likely rapid in this process,<sup>12</sup> it appears that by decreasing the rate of transmetalation and/or reductive elimination one can increase the yield of the B(2) regioisomer (Figure 4B). This type of Pd-catalyzed remote vertex functionalization is unprecedented and demonstrates the utility of a metal-catalyzed route to *meta*-carborane vertex differentiation. Importantly, it contrasts with known thermal rearrangements that are limited to thermally resistant functional groups (above 300 °C) and produce isomer mixtures with B(2) substituted *meta*-carboranes as the minor product.<sup>11</sup>

We attribute this difference in reactivity between “cage-walking” (when using L3) and cross-coupling exclusively at the B(9) vertex (when using L1/L2) to steric crowding at the Pd center. The combination of a sterically demanding ligand and nucleophile appears to inhibit transmetalation,<sup>13</sup> allowing the catalyst to operate through several “cage-walking” steps before re-entering the traditional cross-coupling cycle (vide supra). On the basis of these observations, we propose a Pd-catalyzed “cage-walking” mechanism for isomerization of Br-B(9) (Figure 4B). Beginning with the oxidative addition complex [LPdBr-B(9)], an open Pd(II) coordination site is generated by bromide dissociation<sup>2d</sup> (Figure 4, step II-a) to form [LPd-B(9)]<sup>+</sup>. Consistent with this hypothesis, cross-coupling experiments between Br-B(9) and R3 in the presence of tetrabutylammonium bromide show decreased Br-B(9)

consumption and decreased formation of R3-*meta*-carborane (Figure S7). These experiments suggest that bromide dissociation is an important step in the overall cross-coupling process.<sup>14</sup> After bromide dissociation, two possible “cage-walking” pathways were envisioned for the formally cationic [LPd-B(9)]<sup>+</sup>: (1) deprotonation of an adjacent B-H vertex to form a B(4),B(9)-bound carborane species that isomerizes upon reprotonation to form [LPd-B(4)]<sup>+</sup> (Figure S9) and (2) a Pd-mediated B-H activation that leads to an intramolecular  $\beta$ -hydride shift (Figure S10). Deuterium labeling experiments in which 2,6-Me<sub>2</sub>C<sub>6</sub>H<sub>4</sub>OD was used as the nucleophile did not result in deuterium incorporation at any B-H vertex, as judged by GC-MS and <sup>2</sup>H and <sup>11</sup>B NMR spectroscopy, likely ruling out isomerization pathway 1. However, with the deuterated congener of Br-B(9), 9-Br-10-D-*meta*-C<sub>2</sub>B<sub>10</sub>H<sub>10</sub>, and 2,6-Me<sub>2</sub>C<sub>6</sub>H<sub>4</sub>OH as the nucleophile, we observed five B-<sup>2</sup>H resonances in the <sup>2</sup>H{<sup>11</sup>B} NMR spectrum of R3-B(2), indicating deuterium scrambling across the carborane B-H framework (Figure 4A). We postulate that this  $\beta$ -hydride shift exchanges the B(10) deuterium with an adjacent B(5) proton and enables “cage-walking” to form [LPd-B(4)]<sup>+</sup> (Figure 4B, step II-b). The “cage-walking” process can occur again to generate [LPd-B(2)]<sup>+</sup> (Figure 4B, step II-c). Similar reports of metal-catalyzed carborane B-H activation processes have been reported;<sup>8,15,16</sup> however, they are limited to B-H vertices adjacent to carborane-bound directing groups, whereas the presently reported “cage-walking” accesses all of the *meta*-carborane B-H vertices from one starting point in a diversity-oriented fashion.

Through the “cage-walking” process, the carboranyl fragment eventually binds the Pd center through the most electron-deficient boron vertex, B(2), resulting in a more electrophilic Pd center that can overcome the steric repulsion between the cationic [LPd-B(2)]<sup>+</sup> and the anionic cross-coupling partner. Density functional theory (DFT) calculations (B3LYP/LANL2DZ 6-31G\* and M06/SDD/6-311++G\*\*<sub>SMD</sub>(1,4-dioxane)) on [LPd-B(9)]<sup>+</sup>, [LPd-B(4)]<sup>+</sup>, and [LPd-B(2)]<sup>+</sup> indicate that [LPd-B(2)]<sup>+</sup> has the most cationic Pd center, which likely results in a lower transmetalation barrier due to a stronger electrostatic attraction between the Pd center and the

phenoxide nucleophile (Figures S13–S16). Furthermore, the  $\Delta G$  of B–O and B–N bond formation decreases accordingly,  $B(9) > B(5) \sim B(4) > B(2)$ , for the cross-coupling between Br–B(9) and R1–R3. Similar electronic effects of substrate and ligand were observed in Pd-catalyzed aryl halide cross-coupling.<sup>17</sup>

In summary, we have discovered the first example of metal-catalyzed isomerization (“cage-walking”) of *meta*-carboranyl fragment. The isomerization process appears to operate in conjunction with a classical cross-coupling mechanism, leading to a distribution of carborane regioisomers. The rate of cross-coupling relative to “cage-walking” can be adjusted to achieve selective B-vertex functionalization. We have demonstrated this selectivity by controlling the steric crowding at the Pd center by appropriate choice of catalyst ligand and cross-coupling substrate. Preliminary studies have shown that this “cage-walking” strategy can be applied to carborane B(2)–C<sub>aryl</sub> bond formation using an arylboronic acid (Figure S17). Overall, this approach provides a unique pathway to vertex differentiation of boron clusters.

## ■ ASSOCIATED CONTENT

### Supporting Information

The Supporting Information is available free of charge on the ACS Publications website at DOI: 10.1021/jacs.7b04080.

Full procedures and additional data (PDF)

Crystallographic data (CIF)

## ■ AUTHOR INFORMATION

### Corresponding Author

\*spokoyny@chem.ucla.edu

### ORCID

Yun-Fang Yang: 0000-0002-6287-1640

K. N. Houk: 0000-0002-8387-5261

Alexander M. Spokoyny: 0000-0002-5683-6240

### Notes

The authors declare no competing financial interest.

## ■ ACKNOWLEDGMENTS

We thank the donors of the American Chemical Society Petroleum Research Fund (56562-DNI3 to A.M.S.), UCLA (startup funds to A.M.S.), NSF (CHE-1048804 and CHE1361104), 3M (Non-Tenured Faculty Award to A.M.S.), and the National Defense Science and Engineering Graduate Fellowship Program (to R.M.D.) for support.

## ■ REFERENCES

- (1) (a) Guan, Z.; Cotts, P. M.; McCord, E. F.; McLain, S. J. *Science* **1999**, *283*, 2059–2062. (b) Shultz, L. H.; Brookhart, M. *Organometallics* **2001**, *20*, 3975–3982. (c) Tempel, D. J.; Johnson, L. K.; Huff, R. L.; White, P. S.; Brookhart, M. J. *Am. Chem. Soc.* **2000**, *122*, 6686–6700. (d) Curran, K.; Risse, W.; Hamill, M.; Saunders, P.; Muldoon, J.; Asensio de la Rosa, R.; Tritto, I. *Organometallics* **2012**, *31*, 882–889. (e) Engle, K. M.; Mei, T.-S.; Wasa, M.; Yu, J.-Q. *Acc. Chem. Res.* **2012**, *45*, 788–802.
- (2) (a) Buchwald, S. L.; Nielsen, R. B. *Chem. Rev.* **1988**, *88*, 1047–1058. (b) Hartwig, J. F.; Bergman, R. G.; Andersen, R. A. *J. Am. Chem. Soc.* **1991**, *113*, 3404–3418. (c) Jones, W. M.; Klosin, J. *Adv. Organomet. Chem.* **1998**, *42*, 147–221. (d) Milner, P. J.; Kinzel, T.; Zhang, Y.; Buchwald, S. L. *J. Am. Chem. Soc.* **2014**, *136*, 15757–15766.
- (3) (a) Grotjahn, D. B.; Larsen, C. R.; Gustafson, J. L.; Nair, R.; Sharma, A. *J. Am. Chem. Soc.* **2007**, *129*, 9592–9593. (b) Mei, T.-S.; Patel, H. H.; Sigman, M. S. *Nature* **2014**, *508*, 340–344.

(4) Grimes, R. N. *Carboranes*, 2nd ed.; Elsevier: Oxford, U.K., 2011.

(5) King, R. B. *Chem. Rev.* **2001**, *101*, 1119–1152.

(6) (a) Lugo, C. A.; Moore, C.; Rheingold, A.; Lavallo, V. *Inorg. Chem.* **2015**, *54*, 2094–2096. (b) Joost, M.; Zeineddine, A.; Estévez, L.; Mallet-Ladeira, Miquieu, K.; Amgoune, A.; Bourissou, D. *J. Am. Chem. Soc.* **2014**, *136*, 14654–14657. (c) Douvris, C.; Ozerov, O. V. *Science* **2008**, *321*, 1188–1190. (d) Böhlring, L.; Brockhinke, A.; Kahlert, J.; Weber, L.; Harder, R. A.; Yufit, D. S.; Howard, J. A. K.; MacBride, J. A. H.; Fox, M. A. *Eur. J. Inorg. Chem.* **2016**, *2016*, 403–412. (e) Puga, A. V.; Teixidor, F.; Sillanpää, R.; Kivekäs, R.; Viñas, C. *Chem. Commun.* **2011**, *47*, 2252–2254.

(7) (a) Dash, B. P.; Satapathy, R.; Gaillard, E. R.; Norton, K. M.; Maguire, J. A.; Chug, N.; Hosmane, N. S. *Inorg. Chem.* **2011**, *50*, 5485–5493. (b) Nishino, K.; Yamamoto, H.; Tanaka, K.; Chujo, Y. *Org. Lett.* **2016**, *18*, 4064–4067. (c) Kim, T.; Kim, H.; Lee, K. M.; Lee, Y. S.; Lee, M. H. *Inorg. Chem.* **2013**, *52*, 160–168. (d) Valliant, J. F.; Guenther, K. J.; King, A. S.; Morel, P.; Schaffer, P.; Sogbein, O. O.; Stephenson, K. A. *Coord. Chem. Rev.* **2002**, *232*, 173–230. (e) Issa, F.; Kassou, M.; Rendina, L. M. *Chem. Rev.* **2011**, *111*, 5701–5722. (f) Kennedy, R. D.; Krungleviciute, V.; Clingerman, D. J.; Mondloch, J. E.; Peng, Y.; Wilmer, C. E.; Sarjeant, A. A.; Snurr, R. Q.; Hupp, J. T.; Yildirim, T.; Farha, O. K.; Mirkin, C. A. *Chem. Mater.* **2013**, *25*, 3539–3543. (g) Axtell, J. C.; Kirlikovali, K. O.; Djurovich, P. I.; Jung, D.; Nguyen, V. T.; Munekiyu, B.; Royappa, A. T.; Rheingold, A. L.; Spokoyny, A. M. *J. Am. Chem. Soc.* **2016**, *138*, 15758–15765.

(8) (a) Quan, Y.; Xie, Z. *Angew. Chem., Int. Ed.* **2016**, *55*, 1295–1298. (b) Lyu, H.; Quan, Y.; Xie, Z. *J. Am. Chem. Soc.* **2016**, *138*, 12727–12730.

(9) Dziedzic, R. M.; Saleh, L. M. A.; Axtell, J. C.; Martin, J. L.; Stevens, S. L.; Royappa, A. T.; Rheingold, A. L.; Spokoyny, A. M. *J. Am. Chem. Soc.* **2016**, *138*, 9081–9084 (and references within).

(10) (a) Safronov, A. V.; Kabytaev, K. Z.; Jalisatgi, S. S.; Hawthorne, M. F. *Dalton Trans.* **2014**, *43*, 12467–12469. (b) Bondarev, O.; Sevryugina, Y. V.; Jalisatgi, S. S.; Hawthorne, M. F. *Inorg. Chem.* **2012**, *51*, 9935–9942. (c) Ramachandran, B. M.; Knobler, C. B.; Hawthorne, M. F. *Inorg. Chem.* **2006**, *45*, 336–340.

(11) (a) Kaes, H. D.; Bau, R.; Beall, H. A.; Lipscomb, W. N. *J. Am. Chem. Soc.* **1967**, *89*, 4218–4220. (b) Roscoe, J. S.; Kongpricha, S.; Papetti, S. *Inorg. Chem.* **1970**, *9*, 1561–1563. (c) Kalinin, V. N.; Kobel'kova, N. I.; Zakharkin, L. I. *J. Organomet. Chem.* **1979**, *172*, 391–395.

(12) (a) Marshall, W. J.; Young, R. J., Jr.; Grushin, V. V. *Organometallics* **2001**, *20*, 523–533. (b) Saleh, L. M. A.; Dziedzic, R. M.; Khan, S. I.; Spokoyny, A. M. *Chem. - Eur. J.* **2016**, *22*, 8466–8470.

(13) (a) Sergeev, A. G.; Artamkina, G. A.; Beletskaya, I. P. *Tetrahedron Lett.* **2003**, *44*, 4719–4723. (b) Shen, Q.; Ogata, T.; Hartwig, J. F. *J. Am. Chem. Soc.* **2008**, *130*, 6586–6596. (c) Hicks, J. D.; Hyde, A. M.; Cuezva, A. M.; Buchwald, S. L. *J. Am. Chem. Soc.* **2009**, *131*, 16720–16734. (d) Park, N. H.; Vinogradova, E. V.; Surry, D. S.; Buchwald, S. L. *Angew. Chem., Int. Ed.* **2015**, *54*, 8259–8262.

(14) Fors, B. P.; Davis, N. R.; Buchwald, S. L. *J. Am. Chem. Soc.* **2009**, *131*, 5766–5768.

(15) (a) Qiu, Z.; Ren, S.; Xie, Z. *Acc. Chem. Res.* **2011**, *44*, 299–309 (and references within). (b) Cheng, R.; Qiu, Z.; Xie, Z. *Nat. Commun.* **2017**, *8*, 14827.

(16) (a) Behnken, P. E.; Marder, T. B.; Baker, R. T.; Knobler, C. B.; Thompson, M. R.; Hawthorne, M. F. *J. Am. Chem. Soc.* **1985**, *107*, 932–940. (b) Eleazer, B. J.; Smith, M. D.; Popov, A. A.; Peryshkov, D. V. *J. Am. Chem. Soc.* **2016**, *138*, 10531–10538. (c) Eleazer, B. J.; Smith, M. D.; Peryshkov, D. V. *J. Organomet. Chem.* **2017**, *829*, 42–47.

(17) (a) Hartwig, J. F. *Acc. Chem. Res.* **1998**, *31*, 852–860. (b) Widenhoefer, R. A.; Buchwald, S. L. *J. Am. Chem. Soc.* **1998**, *120*, 6504–6511.